Article

Neuron

Perisaccadic Receptive Field Expansion in the Lateral Intraparietal Area

Highlights

- Receptive fields of LIP neurons expand along the saccadic trajectory
- A model invoking a cortical wave predicts the extent and timing of expansion

Authors

Xiaolan Wang, C.C. Alan Fung, Shaobo Guan, Si Wu, Michael E. Goldberg, Mingsha Zhang

Correspondence

wusi@bnu.edu.cn (S.W.), mingsha.zhang@bnu.edu.cn (M.Z.)

In Brief

Wang et al. found that saccadic remapping in LIP is associated with an expansion of the receptive field along the entire trajectory of the saccade. A cortical wave model of remapping explains this expansion and predicts its extent and timing.

Wang et al., 2016, Neuron *90*, 400–409
April 20, 2016
http://dx.doi.org/10.1016/j.neuron.2016.02.035

CellPress

CellPress

Neuron
Article

Perisaccadic Receptive Field Expansion in the Lateral Intraparietal Area

Xiaolan Wang,[2,7,9] C.C. Alan Fung,[1,3,9] Shaobo Guan,[4] Si Wu,[1,10,*] Michael E. Goldberg,[2,5,6,7,8,10] and Mingsha Zhang[1,10,*]
[1]State Key Laboratory of Cognitive Neuroscience and Learning, IDG/McGovern Institute for Brain Research, Beijing Normal University, Beijing 100875, China
[2]Department of Neuroscience, College of Physicians and Surgeons, Columbia University, New York, NY 10032, USA
[3]Department of Physics, The Hong Kong University of Science and Technology, Clear Water, Hong Kong, China
[4]Department of Neuroscience, Brown University, Providence, RI 02912, USA
[5]Mahoney-Keck Center for Brain and Behavior Research, Department of Neuroscience, College of Physicians and Surgeons
[6]Departments of Neurology, Psychiatry, and Ophthalmology, College of Physicians and Surgeons
[7]Kavli Institute for Neuroscience
Columbia University, New York, NY 10032, USA
[8]Division of Neurobiology and Behavior, New York State Psychiatric Institute, New York, NY 10032, USA
[9]Co-first author
[10]Co-senior author
*Correspondence: wusi@bnu.edu.cn (S.W.), mingsha.zhang@bnu.edu.cn (M.Z.)
http://dx.doi.org/10.1016/j.neuron.2016.02.035

SUMMARY

Humans and monkeys have access to an accurate representation of visual space despite a constantly moving eye. One mechanism by which the brain accomplishes this is by remapping visual receptive fields around the time of a saccade. In this process a neuron can be excited by a probe stimulus in the current receptive field, and also simultaneously by a probe stimulus in the location that will be brought into the neuron's receptive field by the saccade (the future receptive field), even before saccade begins. Here we show that perisaccadic neuronal excitability is not limited to the current and future receptive fields but encompasses the entire region of visual space across which the current receptive field will be swept by the saccade. A computational model shows that this receptive field expansion is consistent with the propagation of a wave of activity across the cerebral cortex as saccade planning and remapping proceed.

INTRODUCTION

Our eyes move constantly, with brief intervals of fixation separated by rapid movements, or saccades. Each saccade changes the retinal location of objects in the world, yet we perceive the world to be stable (Hallett and Lightstone, 1976; Mays and Sparks, 1980). One way that the brain can solve the problem of spatial accuracy is through the phenomenon of predictive remapping of the visual receptive field: neurons in the lateral intraparietal area (LIP) will respond to an object that will be brought into their receptive fields by an impending saccade even before the saccade begins (Duhamel et al., 1992b). This enables neurons to respond in a spatially accurate manner when there is a dissonance between the retinal location of a probe stimulus and vector of the saccade necessary to acquire that probe stimulus. The intensity of the response to a probe stimulus in the presaccadic, or current receptive field (CRF), declines as the cell begins to respond to a probe stimulus in the postsaccadic, or future receptive field (FRF) (Kusunoki and Goldberg, 2003). Before the saccade, however, there is a period of time during which the cell can respond to stimuli in both the CRF and FRF. This phenomenon is equivalent to a transient expansion of the receptive field, and this increase in receptive field size may be responsible for the well-known mislocalization of objects that flash close to the time of saccade (Dassonville et al., 1992; Honda, 1989; Jeffries et al., 2007; Ross et al., 1997). However, it is not known if this paradoxical expansion of the receptive field is limited to the CRF and FRF, or whether the receptive field expands across a larger area of the retina (Figure 1A).

To distinguish among these possibilities, we studied the spatial and temporal features of visual remapping by examining the responses of LIP neurons to a task-irrelevant probe stimulus that appeared briefly before, during, or after a saccade at one of five different spatial locations (Figure 1B): the CRF, the FRF, an intermediate location midway between the two receptive fields (IML), a mirror location of IML across the saccade trajectory (MIML), and a distal location (DL) beyond the FRF into which the receptive field would move if the saccade were larger. We found that immediately before the saccade, LIP neurons respond to stimuli flashed in the space across which the saccade sweeps the retinal receptive field, but not elsewhere in the visual field. The latency of responses for probe stimulus at the IML is shorter than that for probe stimulus at the FRF. We present a computational model of perisaccadic remapping that uses a wave of activity across the cortex to provide a mechanism for remapping. The model predicts the extent and timing of receptive field expansion.

RESULTS

We recorded perisaccadic activity of approximately 100 LIP neurons in one hemisphere of each of two monkeys. Because the results were similar in both monkeys, we pooled the neurons. We

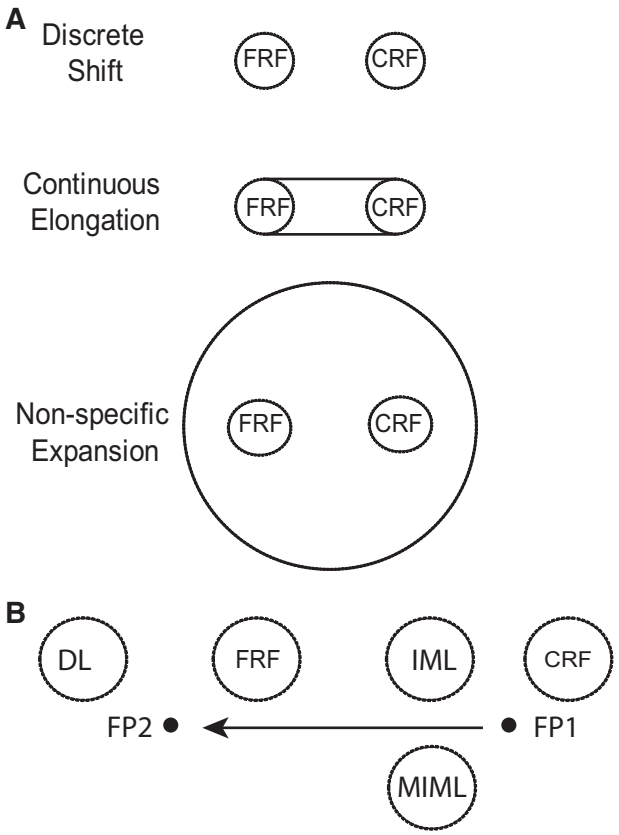

Figure 1. Perisaccadic Receptive Field Expansion in LIP

(A) Possibilities for receptive field expansion. For discrete shift, the cell can be driven by probe stimuli in the CRF and the FRF only. For continuous elongation, the cell can be driven by probe stimuli in the CRF and FRF, and along the retinal trajectory across which the saccade sweeps the receptive field. For nonspecific expansion, the cell can be driven by probe stimuli beyond the limits of continuous elongation.

(B) Experimental design. The monkey makes a saccade from FP1 to FP2. The probe stimuli were placed at one of five spatial locations: CRF; FRF; an intermediate location across which the saccade sweeps the retinal receptive field (IML); a mirror image location reflected across the saccade trajectory from the IML, which is not swept by the retinal receptive field (MIML); and a distal location (DL) extending beyond the FRF in the direction of the saccade, which is not reached by receptive field during the saccade.

first mapped the receptive field of the neurons, either by using a memory-guided saccade task or an automated method in which we flashed stimuli for 50 ms at randomly chosen locations on a 40° × 40° grid (Falkner et al., 2010). We then positioned a fixation point and a saccade target so that the saccade target would not lie in the receptive field of the neuron under study, but the saccade would bring the task-irrelevant probe at FRF into the receptive field. Because LIP receptive fields are large, we usually positioned the saccade target in the ipsilateral visual field, where the saccade would be unable to drive the cell. In our sample, 41 neurons showed remapping, and we studied only these neurons further. For each neuron, we chose three to five possible locations for a task-irrelevant probe stimulus. On each trial, we flashed a probe stimulus for roughly 20–50 ms in one of the five potential probe stimulus locations, chosen pseudorandomly,

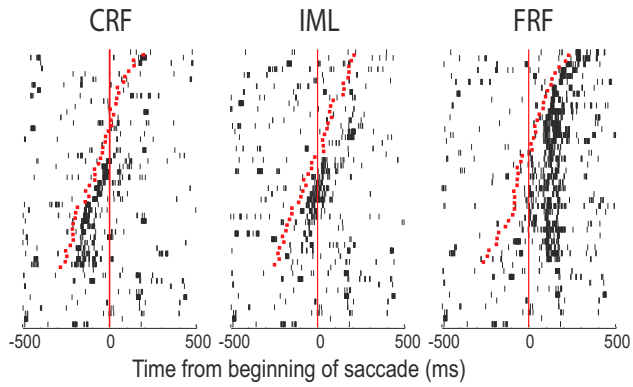

Figure 2. Perisaccadic Expansion of the Receptive Field

Left: probe stimulus in CRF. Each tick is an action potential. The red mark is the time and appearance of the probe stimulus. Trials are synchronized on the beginning of the saccade. Abscissa is the time from beginning of saccade. Successive trials are ranked from bottom to top by the time of appearance of the probe stimulus. At the bottom of each raster are trials in which the probe stimuli did not appear. Center: probe stimulus in IML. Right: probe stimulus in FRF.

at a time from 300 ms before to 300 ms after the fixation point disappeared (Figure 1B). The monkey made the same saccade on every trial, and its saccadic accuracy was not affected by any of the probe stimuli. On 10% of the trials, we did not flash a probe stimulus at all, to assess the eye position and perisaccadic sensitivity of the cell and to ensure that the saccade target itself could not evoke a response from the cell.

As expected, the probe stimulus in the CRF evoked a brisk response when it appeared well before the beginning of the saccade, with a strong phasic and a weaker tonic response. When it appeared at a time closer to the saccade, the tonic response became weaker and stopped at the beginning of the saccade (Figure 2, left panel). The probe stimulus in the IML was outside the cell's CRF and FRF. It failed to evoke a response when it appeared well before or after the saccade began (Figure 2, center panel). However, it started to evoke a response slightly before the saccade began. When the probe stimulus first began to evoke a response in the IML, well before the saccade, the response was time locked to the beginning of the saccade, and when the probe appeared closer to the saccade onset, the response was time locked to the appearance of the probe (Figure 2, center panel). Note that the probe in the FRF evoked a response in the neuron when it appeared before the saccade, and continued to do so after the saccade, when it actually lay in the ordinary receptive field of the neuron.

This pattern of activity holds across most of the population of neurons that we studied. A total of 35/41 neurons had a statistically significant response to the probe in the IML ($p < 0.05$ by Wilcoxon signed-rank). We plotted the spatiotemporal activity of the population as a set of heat maps, with response intensity as a function of time from the beginning of the saccade. Neuronal activity was displayed as color, for 10 ms epochs of the time between the disappearance of the probe stimulus and the beginning of the saccade, ranging from the probe stimulus disappearing between 300 and 290 ms before the saccade to 290 to 300 ms after

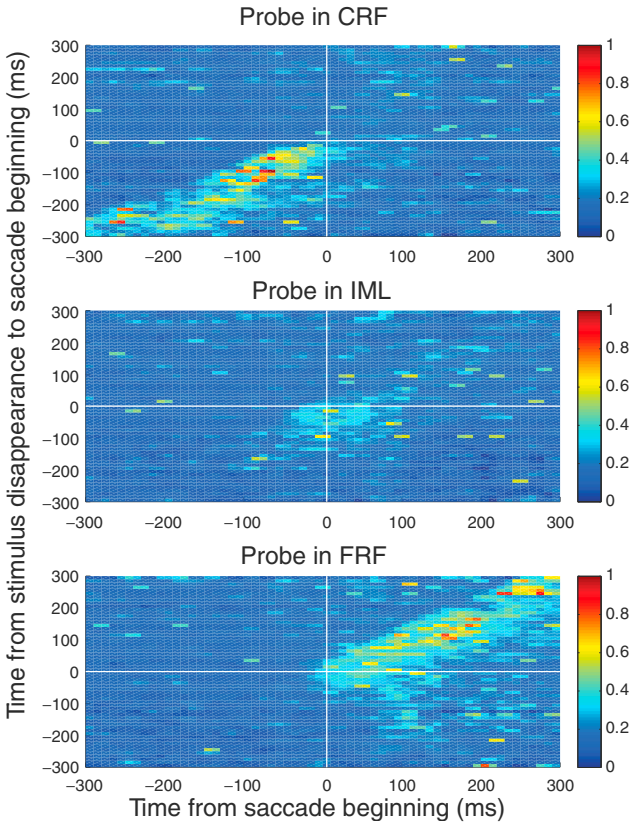

Figure 3. Population Activity of Perisaccadic Responses

Top: probe in CRF. Each line is the average normalized response of the population to probe stimuli during a 10 ms epoch of time. Plotted as a heat map (scale on right) as a function of time from the beginning of the saccade. Bottom row: all trials in which the stimulus disappeared from 300 to 290 ms before the beginning of the saccade. Next row: the stimulus disappeared from 290 to 280 ms. The rows are ordered continuously until the epoch in which the stimulus disappeared from 290 to 300 ms after the beginning of the saccade (top line). Middle panel: probe in IML. Bottom panel: probe in FRF.

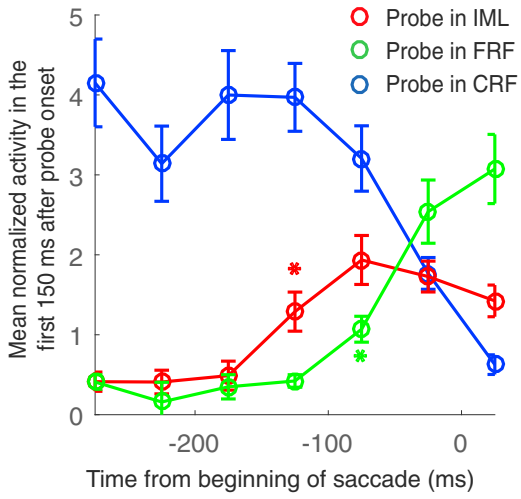

Figure 4. Latency and Intensity Differences of Remapping Responses to Probe Stimuli in CRF, IML, and FRF

Ordinate is normalized activity in the 150 ms after probe onset. Bin width 50 ms. Symbol is at center of bin. The response to the probe in the IML became significantly different from the baseline when the probe appeared 150 to 100 ms before the saccade began ($p < 0.004$, red asterisk), and stayed so until the saccade. The response to the probe in the FRF became significant at 100–50 ms before the saccade ($p < 0.003$, green asterisk) The peak CRF response was significantly stronger than the peak IML response ($p < 0.0002$), which was itself significantly stronger than the FRF response ($p < 0.03$). All comparisons were done by MATLAB Wilcoxon rank-sum. Error bars, SEM.

the saccade (Figure 3). When the probe stimulus appeared in the FRF or IML well before the beginning of the saccade, it did not evoke a response. However, as the probe stimulus appeared closer in time to the saccade, it began to evoke a response. Around the beginning of the saccade, the probe stimulus evoked a response from all three spatial locations.

To study the response to the probe in all three locations quantitatively, we plotted the normalized mean activity in the first 150 ms after the probe onset against time relative to the beginning of the saccade (Figure 4). The IML response became significantly greater than the baseline (activity in the interval 200–150 ms before the probe onset, a time at which activity did not differ as function of probe location, whether the probe appeared in the FRF or the IML) in the interval 150–100 ms before the saccade ($p < 0.003$ by Wilcoxon rank-sum) and remained so until the saccade began, but the FRF response became significant only 100–50 ms before the saccade. Furthermore, the peak CRF response was significantly stronger than the peak IML response ($p < 6 \times 10^{-5}$), which was itself significantly stronger then the FRF response ($p < 0.03$).

The expansion of the receptive field along the trajectory of the saccade was limited to areas of the visual field across which the retinal receptive field swept during the saccade. For 17 neurons, we placed a probe stimulus in a location directly across the saccade trajectory from the IML, the MIML (Figure 1). This location drove the cells little if at all when the monkey looked at the original fixation point or the saccade goal, and, unlike for the IML, stimuli at the MIML evoked little activity in the immediate perisaccadic epoch (Figure S1, available online). Furthermore, the receptive field did not expand beyond the trajectory of the saccade. For 14 cells, we placed the fourth probe location along the same trajectory as the IML but expanded beyond where the FRF would be expected during the saccade, the DL (Figure 1). Probes placed in the DL did not evoke any activity in the neurons (Figure S2).

To understand remapping in the context of receptive field expansion, we designed a computational model in which activity sweeps across the cortex from the representation of the FRF to the representation of the CRF, in a manner similar to a mental rotation. For simplicity, we first present a unidimensional, unidirectional version of the model. Consider a network with two inputs: a set of visual inputs and a set of corollary discharge (CD) inputs representing saccades of different amplitudes in one direction, and an output layer that is equivalent to the LIP priority map (Figure 5). The visual inputs and LIP output neurons share a retinotopic map, such that a visual probe stimulus arriving in the input layer can drive the LIP output neuron. Each output neuron also receives a CD of the saccade. Finally, each neuron in the output layer receives an input from the adjacent neuron whose response field is closer to the FRF than the

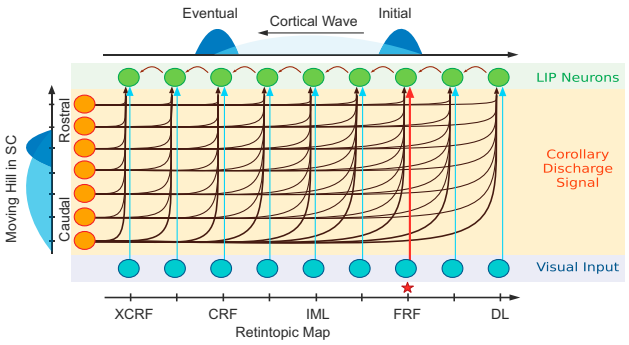

Figure 5. Cartoon of the Model

The model has two input layers, a visual input (blue on bottom) and a CD of the saccade amplitude (orange on left). The LIP priority map output neurons are on the top (green). Each output neuron receives three signals: a visual input that can evoke a response by itself (presumably from V4 or MT), an excitatory input from the adjacent output neuron that cannot drive the neuron by itself, and a CD that also cannot drive the neuron by itself but enables the adjacent cortical neuron to drive the neuron. During remapping, the probe stimulus appears at the FRF location on the retina and drives the output cell. The CD from the saccade enables the FRF cell to excite the adjacent cell, which then can excite the next cell in the cortex, until the wave of excitation reaches the CRF cell. A probe stimulus appearing at the IML location in the retina will excite the CRF cell as a consequence of the remapping of the IML probe stimulus to the XCRF output cell.

CRF. Although the direct visual input can drive the output layer, neither the CD nor the adjacent connections can, by themselves, drive the output layer.

To provide the CD signal, we take advantage of the "moving hill" of saccade activity in the superior colliculus: when a monkey makes a long saccade, activity begins in the intermediate layers of the caudal colliculus with neurons whose movement field describes the actual saccade. As the saccade proceeds, CD activity migrates from the saccade amplitude site toward the rostral colliculus, so that saccadic burst cells with movement fields closer to the center of gaze start to discharge at times closer to the end of saccade, until the rostral colliculus begins to discharge, at which time the saccade ends (Munoz and Wurtz, 1995). The cells with movement fields closer to the fovea discharge when the monkey plans a large saccade, even though the saccade goal does not lie in the movement field of the cell. The cells with small movement fields begin to discharge after the cell whose movement field is the goal of the saccade. We assume that this collicular signal reaches LIP through a disynaptic pathway through the thalamus (Stanton et al., 1977).

During the remapping process, when the probe stimulus appears in the FRF, a neuron whose receptive field lies in the spatial location of the FRF discharges. This neuron is connected to an adjacent cortical neuron whose receptive field lies on a line between the FRF and the CRF (Figure 5). Although the FRF neuron cannot ordinarily excite the adjacent neuron, the presence of the CD signal enables the adjacent neuron to discharge. The second neuron, in turn, projects to an adjacent neuron on the same line, which can now discharge because it is also excited by the CD of the impending saccade. The activity spreads along the cortex until the probe stimulus in the FRF can excite the cell whose receptive field is ordinarily limited to the CRF, as can be seen

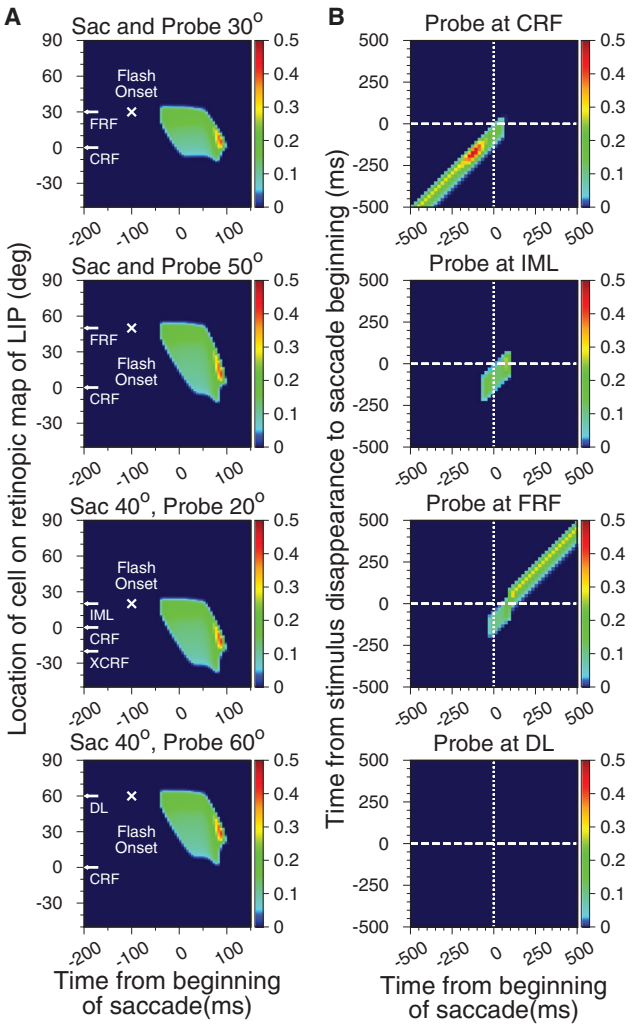

Figure 6. Model Results

(A) Spatiotemporal progression of the wave along the cortex. Each panel plots cortical activity (heat map, scale at right) as a function of the location of the cell in the cortex (ordinate) and the time from the beginning of the saccade (abscissa). We show four different combinations of saccade length and probe location: 30° saccade, probe at 30° on the one-dimensional map; 50° saccade, probe at 50°; 40° saccade, probe at 20°; 30° saccade, probe at 45°. The length of the wave is a function of the saccade amplitude and the probe location.

(B) Response of CRF cell to probes CRF, IML, FRF, and DL. Conventions same as Figure 3; the model duplicates the responses of the cells.

from the instantiation of the model (Figure 6A; sac and probe 30°). When the FRF is farther away from the CRF, the wave proceeds over a larger area of cortex and takes a longer time to complete the remapping process (Figure 6A; sac and probe 50°). The activation of the CRF cell by the IML probe stimulus occurs as a result of the wave. Consider that the IML probe stimulus is in the FRF for a different cell (XCRF). The CRF cell lies between the IML probe stimulus and the XCRF cell, and the wave of excitation excites the CRF cell as a consequence of the remapping of the XCRF cell (Figure 6A; sac 40°, probe 20°). Because the IML cell is closer in the cortex to the CRF cell, a probe stimulus in

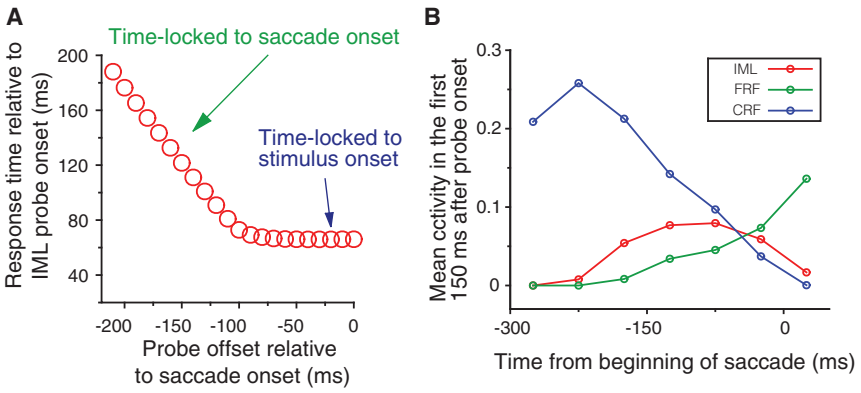

Figure 7. Model Prediction

(A) The model predicts the shift in time locking from saccade onset to stimulus onset. Response time relative to stimulus onset (ordinate) plotted against time from stimulus offset relative to saccade onset (abscissa). When the stimulus appears well before the saccade, the response is time locked to the saccade; when the stimulus appears closer to the saccade, the response is time locked to the stimulus onset.

(B) The model predicts the decrement in response intensity from FRF to IML to CRF. Normalized activity calculated by the model, for the interval from 0 to 150 ms after probe onset (ordinate) plotted against time of stimulus onset relative to saccade onset (abscissa). Each symbol is the average activity in a 50 ms bin. The stimulus lies at the midposition of the bin.

its receptive field will excite the CRF cell before a remapped probe stimulus in the FRF, which is consistent with our data. Similarly, the probe stimulus at DL cannot excite the CRF cell because a wave of excitation initiated by a probe stimulus at DL does not reach the CRF cell (Figure 6A; sac 40°, probe 60°).

The wave model reproduces the spatiotemporal responses of the CRF neurons to probe stimuli at the CRF, intermediate, FRF, and distal locations (compare Figure 6B with Figure 3). Although it was not constrained to do so, the model also reproduces three properties of remapping that we have discovered: (1) the decrease in response latency as the distance from the probe stimulus to the CRF decreases (Figure 6B; compare with Figure 4), (2) the shift in synchrony from saccade to stimulus onset as the stimulus-saccade interval decreases (Figure 7A; compare with Figure 2), and (3) the decrease in the amplitude in the transient response to the probe stimulus as the distance between the probe and the CRF increases (Figure 7B; compare with Figure 4). We present the mathematical details of the model in the Experimental Procedures.

The model as described only works for a single direction of saccade. In order to affect remapping in the opposite direction of saccade, we posit a second group of output neurons that receive CD signals from saccades in the opposite direction, with active lateral connections also in the opposite direction. Output cells sharing a receptive field can mutually excite each other, so that each output cell can report remapping in either direction even though it belongs to a network that only calculates the remapping in one saccade direction (Figure 8A).

Segregating the saccadic inputs renders the problem of expanding the model to a two-dimensional retina relatively trivial. Consider two different scenarios: a remapping of the same cell with a 30° saccade and a 330° saccade (Figure 8B). Although the stimulus in the FRF and the saccade goal (FP2) is the same for each saccade, the beginning fixation points are quite different (FP1a and FP1b), as are the spatial locations of the CRF (CRFa and CRFb). In our model, every output cell in LIP is connected to one direction of CD, but instead of being limited to CDs of opposite directions, as in the unidimensional case, different output cells sharing the same CRF are connected to different CDs covering the entire range of saccade directions, ipsilateral as well as contralateral (Figure 8C). This enables a cell with a given CRF to remap to any spatial location of the FRF in the visual field as long as the combination of saccade and original fixation point are geometrically suitable for the remapping. In the example shown, one unidimensional network receives a set of CD inputs in the direction of saccade A (red curved arrow from the 30° line in the superior colliculus), so when the monkey is looking at FP1a and planning a saccade to FP2, it remaps the stimulus in the FRF easily to the CRF, which occupies the spatial location of CRFa. As the wave proceeds along the cortex, the lateral connections between cells with the same retinotopic receptive field excite the entire population of cells. Thus, although only one network receives the proper CD and has a cortical wave that accomplishes the actual remapping, the remainder of the cells exhibit remapping via the lateral connections. The saccade A network does not receive any CD inputs in the direction of saccade B. When the monkey is looking at FP1b and planning a saccade to FP2, a second network, which receives the CD in the direction of saccade B, remaps the stimulus in the FRF to the CRF, which now occupies the spatial location of CRFb. The lateral connections again excite the cells with the same receptive fields as the cells in the remapping network, but those cells do not participate in the remapping wave. Thus, every cell sharing this receptive field will exhibit an appropriate remapping response for every geometrically appropriate saccade, even though only one unidimensional, unidirectional network performed the actual remapping calculation.

DISCUSSION

Although early studies of the physiology of cortical visual areas assumed that receptive fields were locked to the retina (Wurtz, 1969), more recent studies have shown that this is not always the case. Thus, in V4, retinal locations shift toward the goal of a saccade (Tolias et al., 2001), and toward the locus of the monkey's attention (Connor et al., 1996) even in the absence of a saccade. In particular, many neurons in LIP (Duhamel et al., 1992b), the frontal eye field (FEF) (Umeno and Goldberg, 1997), the prestriate area V3a (Nakamura and Colby, 2002), the parietal reach region (Batista et al., 1999), and the superior colliculus (Walker et al., 1995) show predictive remapping. They shift their receptive fields around the time of a saccade so that a

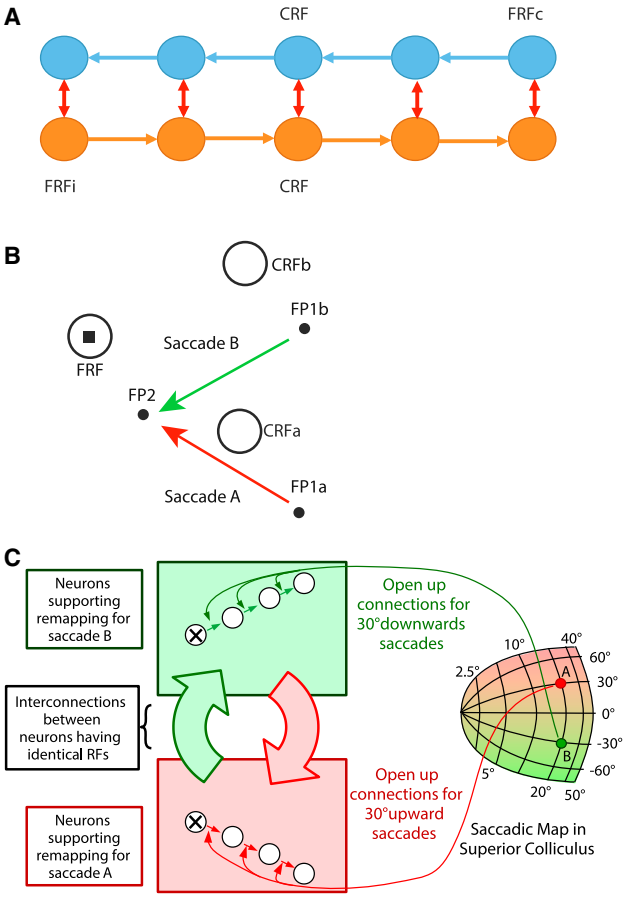

Figure 8. Bidirectional and Two-Dimensional Expansions of the Model

(A) The bidirectional model. Two sets of output neurons are shown, a set receiving a contralateral set of CD inputs (blue) and a set receiving an ipsilateral set of inputs (amber). Neurons with the same receptive fields are connected by mutually excitatory connections, so that neurons participating in an ipsilateral remapping wave can excite neurons that share their receptive field but can only participate in a wave evoked by a contralateral saccade.

(B) Geometry of two-dimensional remapping. Two possible initial fixation points and their related CRFs are shown, FP1a and CRFa, and FP1b and CRFb. When the monkey looks at FP1b, a 30° downward saccade will remap the stimulus in the FRF to the neuron. When the monkey looks at FP1a, a 30° upward saccade will remap the stimulus in the FRF to the same neuron.

(C) The two-dimensional model. The right superior colliculus and two sets of neurons responsible for remapping in two different saccade directions are shown: the upper set receives CDs from 30° downward saccades (green arrows, saccade B in B), the lower set from 30° upward saccades (red arrows, saccade A in B). The visual stimulus at FRF triggers the wave propagation along the path open by the CD signal. Cells with identical receptive fields are connected with excitatory connections, so that a cell excited by a remapping wave evoked by a particular saccade will excite all of the other cells with the same receptive field even though they are not excited by a remapping wave.

probe stimulus that will be brought into their receptive field by the saccade can drive the cell before the saccade, even though the probe stimulus is in a location that would not drive the cell during a fixation task. Furthermore, stimuli that appear and disappear outside the fixation receptive field can evoke a response after a saccade that brings the spatial location of the vanished probe stimulus into the receptive field, even though the cell may not show predictive remapping (Duhamel et al., 1992b; Umeno and Goldberg, 2001).

This study examined the fine structure of the spatial and temporal dynamics of the receptive field shift. We discovered that for predictive shifts, the receptive field expands along the trajectory of the saccade. The receptive field expansion does not occur all at once; probes at the IML evoke a visual response before the probe at the FRF, such that the receptive expands toward the FRF like a rubber band anchored in the CRF. The receptive field does not expand into regions across which the receptive field does not sweep, either for loci between the fixation point and the saccade goal, or for loci beyond the saccade goal.

Because the neurons responded to stimuli that occurred well before the saccade, it is clear that the receptive field change occurs as a result of a CD of the motor command. Sommer and Wurtz (2006) showed that the source of the CD that shifts the receptive fields in the FEF is the superior colliculus, via a signal relayed through the medial dorsal nucleus of the thalamus. The collicular CD signal, however, is not limited to cells whose movement fields lay at the goal of the saccade. Instead, there is a spread of activity from caudal to rostral, such that neurons with movement fields successively closer to the center of gaze fire later. This moving hill of activity was originally suggested to be a mechanism by which activity in the colliculus terminated the saccade by ultimately exciting the fixation zone in the rostral colliculus (Sparks, 1993). However, a band of inactivation across the entire colliculus failed to alter saccade amplitude (Aizawa and Wurtz, 1998), instead only causing a curvature of the saccade. This left no plausible function for the spread of activity in the colliculus, a paradox.

Here we demonstrate a model that takes advantage of a CD of the spread of activity in the colliculus to facilitate a transcortical spread of activity that results in the remapping. The model invokes a spread of activity in the cortex from the static representation of the FRF to the static representation of the CRF, using a CD of the saccade to enable a wave of excitation from the cell that originally responded to the FRF probe stimulus to the CRF cell. The model predicts that a probe stimulus at the IML will drive the CRF cell as a consequence of the transcortical spread of activity evoked by remapping of a probe stimulus from the IML to a cell whose receptive field is at XCRF and in whose receptive field IML will lay after the saccade.

We developed the model to explain remapping with receptive field expansion. The model also explains three other phenomena of receptive field expansion that we had not imposed as constraints of the model, nor had we predicted when we designed the experiment. (1) There are two modes of latency seen in the response to the IML probe: the response to the IML probe is time locked to the saccade when probe appears well before the saccade, but becomes time locked to the probe appearance when the probe appears closer to the saccade (Figure 7A). When the probe stimulus appears well before the saccade, the IML cell begins to discharge, but it cannot excite the adjacent cell until the CD enables the connection, so the response to the IML probe stimulus is synchronized to the saccade onset. When the CD signal arrives before the probe stimulus, the IML activity can excite the adjacent cell from the very first spike because the

corollary signal has already enabled the lateral connection, so the IML response is time locked to the probe appearance. (2) The response to a probe at the IML is greater than the response to a probe at the FRF, and the response to a probe at the CRF is greater than both. The model predicts that the intensity of response would vary with the distance between the CRF and the probe stimulus. (3) The latency of the response to a probe in the IML is less than the latency of the response to a probe in the FRF.

In order to generalize from a unidirectional, one-dimensional model to a bidirectional, one-dimensional model that can remap every saccade, we had to assume that the CD signals were segregated, so that in the set of cells sharing a CRF only one subset was connected to a CD of a particular direction. The cells sharing a CRF excite each other by bidirectional lateral connections, so that although only one subset of cells actually calculated the remapping via a moving wave, all cells sharing the CRF will exhibit remapping for both saccade directions. Because the saccadic signals arise in the contralateral superior colliculus (Wurtz and Goldberg, 1972) and FEF (Bruce and Goldberg, 1985), it is not implausible that this separation between ipsilateral and contralateral saccades be maintained in the cortex, in a manner similar to ocular segregation in layer IV of V1 (Hubel and Wiesel, 1977). In keeping with this idea of segregated inputs, the waveforms for ipsilateral and contralateral saccadic remapping in LIP are not identical (Heiser and Colby, 2006).

The idea that one subset of neuron develops remapping by developing a moving wave via connections from a specific saccade direction, and then transfers activity to cells that share receptive fields but do not participate in the remapping wave, enables an easy generalization of the model to a two-dimensional visual representation that can remap all directions of saccades. We merely assume that the representations of different saccade directions in the colliculus, themselves already segregated, project to different subsets of neurons sharing the same receptive fields in the cortex, and the lateral connections among cells with identical receptive fields excite all the cells that do not actually participate in the remapping calculation.

Previous computational models of receptive field remapping are quite unsatisfactory. One model calculated the remapping by first using an eye position gain field to calculate a craniotopic representation from which remapping could be arrived (Xing and Andersen, 2000). This is unsatisfactory because gain fields are inaccurate for more than 150 ms after a saccade (Xu et al., 2012), a time at which double-step saccades are quite accurate. Another demanded that the entire retina and all directions of saccade project to every LIP neuron (Quaia et al., 1998), which would cause an immensely complicated connectional pattern. Our model eliminates these problems by not requiring gain fields and by requiring that the only visual input to each output neuron is the one necessary to drive its steady-state visual receptive field, and that a given output neuron receives only one direction of saccade and only one connection from an adjacent neuron.

The progression of activity across the cortex has been invoked to explain the time course of mental rotation (Shepard and Metzler, 1971) and the shift of motor plan when a monkey changes the direction of a reach (Georgopoulos et al., 1989). However, the cosine tuning of M1 neurons makes it difficult to prove that the shift actually proceeds by a physical wave of activity moving across the cortex, rather than an averaging of a declining visual response to the target and a rising premotor signal. Other cortical waves have been described in the cerebral cortex, for example, in V1 (Benucci et al., 2007) and V4 (Zanos et al., 2015), but these waves were not associated with specific cognitive processes.

The perisaccadic expansion of the receptive field that we have demonstrated is in conflict with the recent claim by Zirnsak and Moore that the receptive fields of FEF neurons actually remap to a location closer to the fovea than the FRF (Zirnsak et al., 2014). Those authors used a 25 ms flash appearing an average of 69 ms (SD = 35) before the saccade, and averaged activity occurring from 50 to 350 ms after probe onset. By using averaging across such a large interval and lumping activity that occurred before and after the saccade, the authors could not observe the transient receptive field expansion that we have demonstrated. Similarly, because we did not exhaustively examine the spatial tuning of remapping, we cannot exclude some average component of compression of responses toward the saccade goal. Zirnsak and Moore suggested that their results explain the psychophysical compression of visual space toward the fovea for stimuli flashed for 8 ms shortly before the saccade, but this compression does not occur for stimuli flashed more than 50 ms before a saccade (Ross et al., 1997). Furthermore, in Rhesus monkeys, saccades made to stimuli flashed for roughly 50–100 ms before an intervening saccade are not associated with compression toward the fovea at any time (Jeffries et al., 2007), so it is unlikely that the foveal shift could be responsible for compression. Another function claimed for the foveal shift is to facilitate saccade targeting and foveal attention (Zirnsak and Moore, 2014). The authors also claimed that remapping was unlikely to explain the performance of the double-step task. However, inactivation of the medial dorsal nucleus of the thalamus, which impairs both remapping in the FEF (Sommer and Wurtz, 2006) and the accuracy of the second saccade of double-step saccade pairs, does not impair the targeting of the first saccade (Sommer and Wurtz, 2002). A similar finding was demonstrated for patients with parietal lesions (Duhamel et al., 1992a; Heide et al., 1995), who exhibit a slight saccadic hypometria and neglect but exhibit a complete inability to compensate for a saccade into the visual hemifield contralateral to the lesion. The results of these lesion studies support the role of receptive field remapping in generating spatially accurate saccadic eye movements in the double-step task.

One other study has addressed the question of the response to stimuli in IMLs. In an experiment designed to show the importance of the projection to the FEF from the medial dorsal nucleus, Sommer and Wurtz (Sommer and Wurtz, 2006) examined the response to probe stimulus flashed before the saccade at an IML roughly 100 ms before the saccade. In their experiment, unlike ours, the midpoint stimulus appeared in the flank of the CRF (see Figure 2 in Sommer and Wurtz, 2006). Because the cells did not exhibit an increase in their visual responses before the saccade they concluded that the FEF remapped discontinuously. However, the remapping process itself includes not only an expansion of the receptive field to include at least the FRF but also a decrement of response to the stimulus in the CRF (Kusunoki and Goldberg, 2003), as can also be seen in our Figure 4.

If Sommer and Wurtz had chosen IMLs well outside the CRF, they may very well have seen a perisaccadic visual response, especially since there may have been no interplay between CRF suppression and IML enhancement at the midpoint location. Alternatively, the remapping mechanisms in the FEF and LIP might well be entirely different.

EXPERIMENTAL PROCEDURES

Two monkeys (*Macacamulatta*) were used in this experiment. All animal protocols were approved by the New York State Psychiatric Institute and Columbia University Medical Center Institutional Animal Care and Use Committees, which certified their compliance with the NIH Guidelines for the Care and Use of Experimental Animals. During standard sterile surgery under ketamine and isofluorane endotracheal anesthesia, scleral coils, head-restraining devices, and recording chambers were implanted. Chambers were positioned using MRI, and neurons were identified as being in LIP by the consistent visual, memory, and saccade-related response in memory-guided saccade trials to targets in the cell's receptive field (Falkner et al., 2013).

We trained the monkeys to make saccades for liquid reward, using the NIH REX system (Hays et al., 1982) for behavioral control and data collection, running on a Dell Optiplex PC under the QNX real-time operating system. We used two different methods for stimulus presentation. In early experiments, we used a 22-in Mitsubishi monitor (resolution of 1,024 × 768, with refresh frequency of 100 HZ) running the Vex open GL-based graphics system (available by download from lsr-web.net). In these experiments, we determined the time of probe stimulus presentation from the vertical refresh of the monitor. The monitor phosphor had a decay rate of less than 2 ms as measured by a Minolta photometer, and a dark-adapted human observer saw no persistence of the image after a saccade. In later experiments, we used a Hitachi LCD projector with a frame refresh rate of 60 Hz to display stimuli on a tangent screen. Because the feedback signal from this projector is not reliable, we used a photocell to record the actual time of probe stimulus appearance and disappearance. We found no difference in the time course of neuronal responses between experiments using the different visual display methods. We measured eye position using subconjunctivally implanted search coils (Judge et al., 1980) and either a Riverbend phase detector (for the monitor experiments) or a Northmore phase detector (Crist Associates), at a sampling frequency of 1 KHz.

We recorded neurons using glass-coated tungsten electrodes (Alpha Omega) or multibarrel pipette with a central tungsten recording electrode, and commercially available amplification (FHC or Alpha Omega) and filtering (Krohn-Hite) equipment (Falkner et al., 2013). We first mapped the receptive field of the neurons, either by using a memory-guided saccade task or an automated method in which we flashed stimuli for 50 ms at randomly chosen locations on a 40° × 40° grid (Falkner et al., 2010). We then positioned a fixation point and a saccade target so that the saccade target would not be in the receptive field of the neuron under study, but the saccade would bring a task-irrelevant probe at the FRF into the receptive field. We did all data analysis with MATLAB.

The Computational Model Structure

We present a one-dimensional network model formed by LIP neurons that accomplishes predictive remapping in a single direction. The model can be easily extended to achieve bidirectional remapping or remapping in the two-dimensional space as described in the main text. As shown in Figure 5, neurons are aligned according to their receptive field locations in retinotopic coordinates. In the simulation, we consider N = 256 neurons that are uniformly distributed in the range of (−120°, 120°). We make the assumption that the firing rate of a neuron at position x_i is determined by $u(x_i, t)$, its synaptic current (Wilson and Cowan, 1973).

The synaptic current is determined by its own relaxation, inputs from other neurons in LIP, CD signal, and the visual input. It is given by

$$\tau_s \frac{du(x_i,t)}{dt} = -u(x_i,t) + [J_{i,i+1} r(x_{i+1})] I^{CD}(t - \tau_{CD,lat}) + I^V(x_i,t), \quad \text{(Equation 1)}$$

where $\tau_s = 1$ ms is the time constant of synaptic current and $\tau_{CD,lat} = 10$ ms is the transmission latency of the CD signal. $J_{i,i-1} = 1$ is the connection between two adjacent neurons, I^V is the current provided by the visual input (Figure S3A), and I^{CD} is the current provided by the CD input (Figure S3B). The firing rate of the neuron is a sigmoidal function of the current,

$$r(x_i,t) = \frac{\tanh[u(x,t) - \theta_r]\Theta[u(x_i,t) - \theta_r]}{S(t)}, \quad \text{(Equation 2)}$$

where $\Theta(x)$ is a step function, i.e, $\Theta(x) = x$, for $x > 0$, and $\Theta(x) = 0$, for $x \leq 0$. θ_r is the firing threshold, above which the sum of inputs can activate a neuron. We choose $\theta_r = 0.2$.

A second function of the CD is to suppress the response of the CRF cell to the CRF probe stimulus at the beginning of the remapping process (Kusunoki and Goldberg, 2003). Function $S(t)$ models the saccadic suppression effect:

$$S(t) = \begin{cases} \left\{1 + k \exp\left[-\frac{1}{2}\left(\frac{t}{66\ \text{ms}}\right)^2\right]\right\}^{-1} & t < 0\ ms \\ \left\{1 + k \exp\left[-\frac{1}{2}\left(\frac{t}{62\ \text{ms}}\right)^6\right]\right\}^{-1} & t \geq 0\ \text{ms}, \end{cases} \quad \text{(Equation 3)}$$

where k is the parameter for the saccadic suppression, which we choose to be 4.0. This particular choice of k is chosen to balance the magnitudes of CD signal we used.

The only visual input that can drive a neuron in the model is the visual input to the cell in whose receptive field the FRF probe stimulus lies: the FRF cell. All other cells are driven by the CD-augmented signal from the adjacent neuron.

As the mathematical model we proposed here is highly nonlinear, an analytic solution cannot be obtained. We solve $r(x_i, t)$ by using a numerical method; the Dormand-Prince method provided by the GNU scientific library is used to integrate Equation 1 for various probe stimulus onset time and offset time. The Dormand-Prince method is a member of the Runge-Kutta family of solvers, which is applicable to various differential equations. All numerical calculations are done using Intel Ivy-bridge class processors.

Since the focus of the present study is to illustrate a potential mechanism to generate predictive remapping, we only consider a one-dimensional model for neurons located along the saccadic direction. We consider a saccade that is from left to right.

$I^V(x_i, t)$ is the visual input representing the probe stimulus, which is given by

$$I^V(x_i,t) = \begin{cases} A^V exp\left\{-\frac{[x_i - z_0(t - \tau_{delay})]^2}{2a_i^2}\right\} & for\,(t - \tau_{delay}) \in [t_{on}, t_{off}] \\ A^V exp\left[-\frac{t - \tau_{\text{delay}} - t_{\text{off}}}{100\ \text{ms}}\right] exp\left\{-\frac{[x_i - z_0(t - \tau_{delay})]^2}{2a_i^2}\right\} & for\,(t - \tau_{delay}) > t_{off} \\ 0 & otherwise, \end{cases} \quad \text{(Equation 4)}$$

where $\tau_{delay} = 50$ ms is the visual transmission delay from retina to LIP. t_{on} and t_{off} are the onset and offset moments of the probe stimulus. z_0 is the retinotopic location of the probe stimulus, which can be CRF, IML, FRF, or DL. A^V is the input strength, which equals to 0.5. We choose the parameter $a_I = 5°$, so that I^V covers a range of 20° (Figure S3A), which is about the receptive field size of LIP neurons observed in the experiment.

$I^{CD}(t)$ is the CD signal originating from the moving hill activity in the superior colliculus (Munoz and Wurtz, 1995) (Figure 5). Without loss of generality, we set $t = 0$ the onset time of a saccade. I^{CD} is given by

$$I^{CD}(t) = \begin{cases} A^{CD} \exp\left[-\frac{1}{2}\left(\frac{t}{75\ \text{ms}}\right)^2\right] & t < 0\ ms \\ A^{CD} \exp\left[-\frac{1}{2}\left(\frac{t}{65\ \text{ms}}\right)^6\right] & t \geq 0\ \text{ms}, \end{cases} \quad \text{(Equation 5)}$$

where A^{CD} is the strength of the CD signal. The CD signal appears around 100–200 ms before saccade, but a significant fraction of the collicular burst cells stop firing by the end of the saccade (Waitzman et al., 1991), so we have used the asymmetric time course of the superior colliculus partially clipped cells as the CD (Figure S3B). The exact duration of the CD signal is not crucial in our model. The strength of the CD signal depends on the magnitude of the saccade. The dependence of A^{CD} on saccadic magnitude is not explicitly specified. However, the range of remapping is a monotonic function of A^{CD}. From this, one may match a value of A^{CD} to a magnitude of saccade. For instance, in Figure 6, A^{CD} for a 30° saccade is 7.30 nA, A^{CD} for a 40° saccade is 7.37 nA, and A^{CD} for a 50° saccade is 7.38 nA.

SUPPLEMENTAL INFORMATION

Supplemental Information includes three figures and can be found with this article online at http://dx.doi.org/10.1016/j.neuron.2016.02.035.

AUTHOR CONTRIBUTIONS

M.E.G., M.Z., and X.W. designed the experiment and analyzed the experimental data. X.W., C.C.A.F., and M.E.G. made the figures. M.Z. and X.W. did the physiological recording. S.G., S.W., C.C.A.F., M.Z., and M.E.G. developed the model. All authors contributed to writing the paper.

ACKNOWLEDGMENTS

This work was partially supported by National Natural Science Foundation of China (31471069, 91432109, and 31261160495); 973 program (2011CBA00406 and 2014CB846101) of Ministry of Science and Technology of China; the Research Grants Council of Hong Kong (604512, 605813, and N_HKUST 606/12); and by grants from the Zegar, Keck, Kavli, and Dana Foundations, and the National Eye Institute (P30EY019007, R01EY014978, and R01EY017039, to M.E.G., PI), We are grateful to Yana Pavlova and Suzi Kriminska for veterinary technical help; Drs. Girma Asfaw and Moshe Shalev for veterinary care; John Caban and Matthew Hasday for machining; Glen Duncan for computer and electronic assistance; and Latoya Palmer, Cherise Washington, and Holly Kline for facilitating everything. Dr. Robert Wurtz and Dr. Marc Sommer read an earlier version of the manuscript.

Received: August 20, 2015
Revised: January 27, 2016
Accepted: February 19, 2016
Published: March 31, 2016

REFERENCES

Aizawa, H., and Wurtz, R.H. (1998). Reversible inactivation of monkey superior colliculus. I. Curvature of saccadic trajectory. J. Neurophysiol. *79*, 2082–2096.

Batista, A.P., Buneo, C.A., Snyder, L.H., and Andersen, R.A. (1999). Reach plans in eye-centered coordinates. Science *285*, 257–260.

Benucci, A., Frazor, R.A., and Carandini, M. (2007). Standing waves and traveling waves distinguish two circuits in visual cortex. Neuron *55*, 103–117.

Bruce, C.J., and Goldberg, M.E. (1985). Primate frontal eye fields. I. Single neurons discharging before saccades. J. Neurophysiol. *53*, 603–635.

Connor, C.E., Gallant, J.L., Preddie, D.C., and Van Essen, D.C. (1996). Responses in area V4 depend on the spatial relationship between stimulus and attention. J. Neurophysiol. *75*, 1306–1308.

Dassonville, P., Schlag, J., and Schlag-Rey, M. (1992). Oculomotor localization relies on a damped representation of saccadic eye displacement in human and nonhuman primates. Vis. Neurosci. *9*, 261–269.

Duhamel, J.-R., Goldberg, M.E., Fitzgibbon, E.J., Sirigu, A., and Grafman, J. (1992a). Saccadic dysmetria in a patient with a right frontoparietal lesion. The importance of corollary discharge for accurate spatial behaviour. Brain *115*, 1387–1402.

Duhamel, J.R., Colby, C.L., and Goldberg, M.E. (1992b). The updating of the representation of visual space in parietal cortex by intended eye movements. Science *255*, 90–92.

Falkner, A.L., Krishna, B.S., and Goldberg, M.E. (2010). Surround suppression sharpens the priority map in the lateral intraparietal area. J. Neurosci. *30*, 12787–12797.

Falkner, A.L., Goldberg, M.E., and Krishna, B.S. (2013). Spatial representation and cognitive modulation of response variability in the lateral intraparietal area priority map. J. Neurosci. *33*, 16117–16130.

Georgopoulos, A.P., Lurito, J.T., Petrides, M., Schwartz, A.B., and Massey, J.T. (1989). Mental rotation of the neuronal population vector. Science *243*, 234–236.

Hallett, P.E., and Lightstone, A.D. (1976). Saccadic eye movements to flashed targets. Vision Res. *16*, 107–114.

Hays, A.V., Richmond, B.J., and Optican, L.M. (1982). A UNIX-based multiple process system for real-time data acquisition and control. WESCON Conf Proc *2*, 1–10.

Heide, W., Blankenburg, M., Zimmermann, E., and Kömpf, D. (1995). Cortical control of double-step saccades: implications for spatial orientation. Ann. Neurol. *38*, 739–748.

Heiser, L.M., and Colby, C.L. (2006). Spatial updating in area LIP is independent of saccade direction. J. Neurophysiol. *95*, 2751–2767.

Honda, H. (1989). Perceptual localization of visual stimuli flashed during saccades. Percept. Psychophys. *45*, 162–174.

Hubel, D.H., and Wiesel, T.N. (1977). Ferrier lecture. Functional architecture of macaque monkey visual cortex. Proc. R. Soc. Lond. B Biol. Sci. *198*, 1–59.

Jeffries, S.M., Kusunoki, M., Bisley, J.W., Cohen, I.S., and Goldberg, M.E. (2007). Rhesus monkeys mislocalize saccade targets flashed for 100ms around the time of a saccade. Vision Res. *47*, 1924–1934.

Judge, S.J., Richmond, B.J., and Chu, F.C. (1980). Implantation of magnetic search coils for measurement of eye position: an improved method. Vision Res. *20*, 535–538.

Kusunoki, M., and Goldberg, M.E. (2003). The time course of perisaccadic receptive field shifts in the lateral intraparietal area of the monkey. J. Neurophysiol. *89*, 1519–1527.

Mays, L.E., and Sparks, D.L. (1980). Saccades are spatially, not retinocentrically, coded. Science *208*, 1163–1165.

Munoz, D.P., and Wurtz, R.H. (1995). Saccade-related activity in monkey superior colliculus. II. Spread of activity during saccades. J. Neurophysiol. *73*, 2334–2348.

Nakamura, K., and Colby, C.L. (2002). Updating of the visual representation in monkey striate and extrastriate cortex during saccades. Proc. Natl. Acad. Sci. USA *99*, 4026–4031.

Quaia, C., Optican, L.M., and Goldberg, M.E. (1998). The maintenance of spatial accuracy by the perisaccadic remapping of visual receptive fields. Neural Netw. *11*, 1229–1240.

Ross, J., Morrone, M.C., and Burr, D.C. (1997). Compression of visual space before saccades. Nature *386*, 598–601.

Shepard, R.N., and Metzler, J. (1971). Mental rotation of three-dimensional objects. Science *171*, 701–703.

Sommer, M.A., and Wurtz, R.H. (2002). A pathway in primate brain for internal monitoring of movements. Science *296*, 1480–1482.

Sommer, M.A., and Wurtz, R.H. (2006). Influence of the thalamus on spatial visual processing in frontal cortex. Nature *444*, 374–377.

Sparks, D.L. (1993). Are gaze shifts controlled by a 'moving hill' of activity in the superior colliculus? Trends Neurosci. *16*, 214–218.

Stanton, G.B., Cruce, W.L.R., Goldberg, M.E., and Robinson, D.L. (1977). Some ipsilateral projections to areas PF and PG of the inferior parietal lobule in monkeys. Neurosci. Lett. *6*, 243–250.

Tolias, A.S., Moore, T., Smirnakis, S.M., Tehovnik, E.J., Siapas, A.G., and Schiller, P.H. (2001). Eye movements modulate visual receptive fields of V4 neurons. Neuron *29*, 757–767.

Umeno, M.M., and Goldberg, M.E. (1997). Spatial processing in the monkey frontal eye field. I. Predictive visual responses. J. Neurophysiol. *78*, 1373–1383.

Umeno, M.M., and Goldberg, M.E. (2001). Spatial processing in the monkey frontal eye field. II. Memory responses. J. Neurophysiol. *86*, 2344–2352.

Waitzman, D.M., Ma, T.P., Optican, L.M., and Wurtz, R.H. (1991). Superior colliculus neurons mediate the dynamic characteristics of saccades. J. Neurophysiol. *66*, 1716–1737.

Walker, M.F., Fitzgibbon, E.J., and Goldberg, M.E. (1995). Neurons in the monkey superior colliculus predict the visual result of impending saccadic eye movements. J. Neurophysiol. *73*, 1988–2003.

Wilson, H.R., and Cowan, J.D. (1973). A mathematical theory of the functional dynamics of cortical and thalamic nervous tissue. Kybernetik *13*, 55–80.

Wurtz, R.H. (1969). Response of striate cortex neurons to stimuli during rapid eye movements in the monkey. J. Neurophysiol. *32*, 975–986.

Wurtz, R.H., and Goldberg, M.E. (1972). Activity of superior colliculus in behaving monkey. 3. Cells discharging before eye movements. J. Neurophysiol. *35*, 575–586.

Xing, J., and Andersen, R.A. (2000). Memory activity of LIP neurons for sequential eye movements simulated with neural networks. J. Neurophysiol. *84*, 651–665.

Xu, B.Y., Karachi, C., and Goldberg, M.E. (2012). The postsaccadic unreliability of gain fields renders it unlikely that the motor system can use them to calculate target position in space. Neuron *76*, 1201–1209.

Zanos, T.P., Mineault, P.J., Nasiotis, K.T., Guitton, D., and Pack, C.C. (2015). A sensorimotor role for traveling waves in primate visual cortex. Neuron *85*, 615–627.

Zirnsak, M., and Moore, T. (2014). Saccades and shifting receptive fields: anticipating consequences or selecting targets? Trends Cogn. Sci. *18*, 621–628.

Zirnsak, M., Steinmetz, N.A., Noudoost, B., Xu, K.Z., and Moore, T. (2014). Visual space is compressed in prefrontal cortex before eye movements. Nature *507*, 504–507.